Fermilab

TM-1431
1100.400

Muon Calculations for the Polarized Proton Beamline

J. D. Cossairt

November 1986

TM-1431

1100.400

MUON CALCULATIONS FOR THE POLARIZED PROTON BEAMLINE

J. D. Cossairt

November, 1986

1. Introduction

The new polarized proton beam (MP), presently being installed in the Meson Area is of unique design. Being a beamline totally above grade, the fluence of muons emitted is of great interest for both radiation protection and experimental background considerations. This note reports on Monte-Carlo calculations of the muon intensities due to this beam using the program CASIM. These results should be straightforward to test experimentally during the upcoming Tevatron fixed target physics run.

2.Geometry and Method of Calculation

Figures 1-7 illustrate the geometry of the MP beamline approximately as it was modeled in the Monte-Carlo calculations and define the coordinate system used. This beam is unique in that the polarized protons are actually a tertiary beam. The incident primary protons are swept downward by standard target pile sweeping magnets into the copper beam dump. Neutral particles, among them Λ's, are allowed to go forward at zero degrees through the beam dump. The Λ's then decay into the polarized protons (which are not considered further in the present analysis of muon fluences). All beam which is able to pass through the magnet apertures then eventually reaches the neutral dump which is aligned so that the neutrals strike the brass insert in the gap of the BM105's while the tertiary beam of polarized protons (or antiprotons) is transported through an unobstructed portion of the gap below the insert. The names of the magnets in this beamline are standard Fermilab designations; a detailed illustration of a BM105 is included because of its unusually large size. These magnets are used because a large aperture is necessary to capture significant numbers of the tertiary polarized protons. Their large cross section also enhances their effect upon halo muons relative to that of smaller, more typical beam transport dipoles.

The program CASIM (Va75a) has been quite generally used for hadron shielding calculations

and tested for large geometries (Co82, Co85). A rather elderly FN reports on its usage for calculation of muon radiation fields (Va75b). Recently, Van Ginneken has improved it substantially for this purpose and this upgraded version, with its more correct treatment of muon production and energy deposition processes (Va86) , is used in the calculations reported here. A limited experimental test of this program for a somewhat similar geometry has been documented elsewhere (Co86). As always, the geometry is specified by means of a FORTRAN subroutine and can be done to any degree of detail desired. This program does a complete model of the hadronic cascade and explicitly follows protons, pions and neutrons. Muons are generated throughout the cascade as appropriate. Thus muons from the beam dump and associated shielding are included as well as those produced by the production target. The production mechanisms considered include those due to the decays of pions and kaons (expected to dominate at Tevatron energies), prompt production, and pair production by photons. The muons thus produced are then followed throughout the remainder of the geometry until they are leave the boundaries or are ranged out. The present author has set up a binning scheme by quadrants (illustrated in the figures) which is necessary because of the expected azimuthal asymmetries due to the bending by magnetic fields. In this scheme, the muons were "counted" as they traversed specified vertical planes, perpendicular to the longitudinal axis, Z.

Figures 1-7 are schematic in intent; the actual dimension of components were modeled in the calculations. Magnetic fields were included exactly in the gaps of the dipoles at values appropriate to the presently planned operation with 200 GeV/c polarized protons. Yoke fields in dipoles were approximated by resorting to intuitive notions about field direction and flux conservation expressed in simple formulae. Quadrupole fields were not included, but the iron of the quadrupoles was included in the model.

The calculations were done in two stages. First, areas upstream of the shielding hill were modeled with a steplength of 50 cm to track the muons. Such a short steplength makes for rather slow tracking but preserves accuracy. To follow the muons downstream of the shielding hill in a reasonable amount of computer time, a much coarser steplength of 500 cm was used.

3. Results of Calculations

In the results presented in this section, tissue absorbed dose per incident proton (mrad/proton) is reported. According to Stevenson (St84), a conversion of 25,000 muons/cm^2 per mrad is appropriate. Therefore, this factor can be used by those desiring the actual muon fluence or flux density. Hence, 1 X 10^{-15} mrad per incident proton, if received during a 20 second long uniform beam spill of 3 X 10^{12} incident primary protons would represent a flux density of 3.75

muons/(cm^2-sec). The same normalized absorbed dose would result in an hourly absorbed dose rate of 0.18 mrad/hr, if 60 spills per hour at this intensity were ttargeted. This is a plausible operating scenario during data-taking of E704.

Plots of all 4 quadrants are shown together in a rather unconventional format. Figures 8 and 9 show the predictions under normal operating conditions of the beam line. Figure 8 shows them plotted in each of the four quadrants at each of three different Z-values for the shorter steplength used upstream of the shielding hill. In each plot,the results using more than one random initial value ("seed") is shown. The differences between the seeds may be taken as the error in the calculation in that particular radial bin. Such variations are primarily due to the expected statistical errors in the calculations which were arbitrarily limited to about 6000 CPU seconds on the CYBER for each run with a given "seed". Figure 9 shows the predicted distributions for the coarse steplength at two locations. As one can see, the agreement at Z=295 between the two calculations is adequate for radiation protection purposes; the primary intent of calculations carried out to rather large radii (20m). In these figures, it is obvious that the configuration of the dipoles as vertical bends results in much higher dose rates above ground (quadrant 2) than at the surface. The results in the downward quadrant (quadrant 3) show the effect of the presence of the earth. Typical dose rates away from the beam axis (e.g., for R > 600 cm) in the horizontal plane (in quadrants 1 and 4) at 3 X 10^{12} protons per spill, 60 spills per hour are predicted to range from 0.18 down to 0.018 mrad/hr. Beyond the shielding hill, at Z=590 m , the dose rates are predicted to be a maximum of 0.009 mrad/hr "on axis" and at least an order of magnitude lower "off axis" at the beam level. The shielding hill clearly is very effective in reducing these muon intensities.

A number of calculations were also carried out for a more restricted radial space (R< 5 m) to obtain more detailed information near the beam axis and to test various parts of the model used. Figure 10 shows the results at several values of Z for normal operating conditions. This compares well with those shown in Figure 8 using much larger radial bins. Figure 11 shows the effects of removing the earth berm from the model (the ground beneath was, however, still included). It is seen that the earth berm is of some utility in reducing the muon fluences at radii where it "shadows" areas downstream.

Figure 12 involves normal operating conditions but without magnetic fields turned on in any of the dipoles in the beam line. This is an unlikely possible running mode, but shows the effects of the muon sweeping by these magnets. Figure 13 has all dipoles turned "on" except the first sweeping magnet in the target pile, while Figure 14 has both target pile sweeping magnets turned "off", but with all other beamline dipoles "on". The latter is a conceivable running mode; it may be necessary

to assure adequate focussing of the secondary beam to accomplish proper selection of the polarized protons. Both in this instance, and that shown in Fig. 12, the primary proton beam is effectively disposed of in the neutral dump. In Fig. 15, the target pile sweeping magnets are "on "while all of the dipoles downstream are turned "off". Figure 16 shows the results obtained when the target is removed. As one can see, differences at small radii with and without the target are quite small. This implies that the muons seen at the experiment arise predominately from the shower in the beam dump and would be neglicted entirely in calculations in which muonsare produced at the production target only.

Values of momentum spectra at various values of Z averaged over "seed" in each of four radial bins for three values of Z are listed in Table 1. Here it is seen, as expected that the average muon momentum at the larger radii generally increases as Z increases. Obviously, the enormous flood of low energy muons produced in the beam dump is gradually reduced by magnetic deflection and energy loss mechanisms in the iron of the magnets and the earth shielding as they proceed down the beamline.

4 Conclusion

It is hoped that the results presented here will serve as a guide to both experimenters and radiation safety personnel who are preparing for initial operation of this beamline. These results should be easy to check during its initial operation.

References

Co82 J. D. Cossairt, N. V. Mokhov, and C. T. Murphy, "Absorbed Dose Measurements External to Thick Shielding at a High Energy Proton Accelerator: Comparison with Monte-Carlo Calculaitons", Nucl. Instr. and Meth 197 (1982) 465.

Co85 J. D. Cossairt, S. W. Butala, and M. A. Gerardi, "Absorbed Dose Measurements at an 800 Gev Proton Accelerator: Comparison with Monte-Carlo Calculations", Nucl. Instr. and Meth. A238 (1985) 504.

Co86 J. D. Cossairt, "Shielding Design at Fermilab; Calculations and Measurements", submitted to the proceedings of the Twentieth Midyear Topical Symposium of the Health Physics Society: Health Physics of Radiation Producing Machines, Reno Nev. February 1987, FERMILAB-CONF-86/156..

St84 G. R. Stevenson, "Dose and Dose Equivalent from Muons", CERN Report TIS-RP/099, 1984.

Va75a A. Van Ginneken, "CASIM; Program to Simulate Transport of Hadronic Cascades in Bulk Matter", Fermilab Report FN-272, 1975 and A. Van Ginneken and M. Awschalom, High Energy Partical Interactions in Large Targets: Volume 1, Hadronic Cascades, Shielding, Energy Deposition, Fermilab, Batavia, IL 60510, 1975.

Va75b A. Van Ginneken,"Penetration of Prompt and Decay Muon Components of Hadronic Cascades Through Thick Shields", TM-630, 1975.

Va86 A. Van Ginneken, "Energy Loss and Angular Characteristics of High Energy Electromagnetic Processes", Nucl. Instr. and Meth. A251 (1986) 21.

Table 1

AVERAGE MOMENTA (GeV/c) IN SEVERAL RADIAL BINS

UNDER NORMAL OPERATING CONDITIONS

Z(meters)	R<50 cm	50<R<100cm	100<R<200cm	R>200cm
75	22.7±6.6	39.1±3.6	47.5±2.2	18.2±4.5
150	120.4±5.1	85.8±4.9	60.6±20.4	38.4±5.2
225	102.6±14.8	91.5±2.9	71.8±4.4	27.5±1.4
295	96.4±3.0	102.6±10.9	79.5±14.7	61.5±1.9

List of Figure Captions

1. Plan view of the MP beam in the plane of the beam. The various elements are indicated schematically as denoted in the legend. Both transverse (X) and longitudinal (Z) scales are only approximate in this figure. The 12 most upstream BM105's will normally operate with gap fields of 1.4 T while the remainder will have gap fields of 1.5 T.

2. Cross section of the MP beam at the target pile, approximately as modeled, in the region of the sweeping magnets at Z = 8 meters.

3. Cross section of the MP beam, approximately as modeled, at Z = 70 meters (at the neutral dump).

4. Cross section of the MP beam, approximately as modeled, at Z = 90 meters (in a random section of beam transport enclosure.

5. Longitudinal vertical section of the MP beam in its plane showing the experimental hall and the shielding hill (Mt. Taijji).

6. Detailed view of the iron final beam dump imbedded in the upstream end of the shielding hill.

7. Detailed view of a BM105 magnet as used in the MP beamline.

8. Plots of absorbed dose as a function of radius R for each quadrant at various Z values. Normal operating conditions prevail here.

9. Similar to Figure 8 for two Z-values, except that these are for the extra long steplength. Normal operating conditions prevail here.

10. Similar to Figure 8 except that a smaller maximum radial dimension is considered. Normal operating conditions prevail here.

11. Results obtained with the earth berm removed.

12. Results obtained at Z = 295 meters with all magnetic fields turned "off".

13. Results obtained at Z = 295 meters with all magnetic fields turned "on" except that of the initial target pile sweeping magnet.

14. Results obtained at Z = 295 meters with the sweeping magnets turned off but with all beamline dipoles turned "on".

15. Results obtained at Z=295 meters with the sweeping magnets "on" but with all beamline dipoles turned "off".

16. Results obtained at Z=295 meters with normal operating conditions except that the target has been removed.

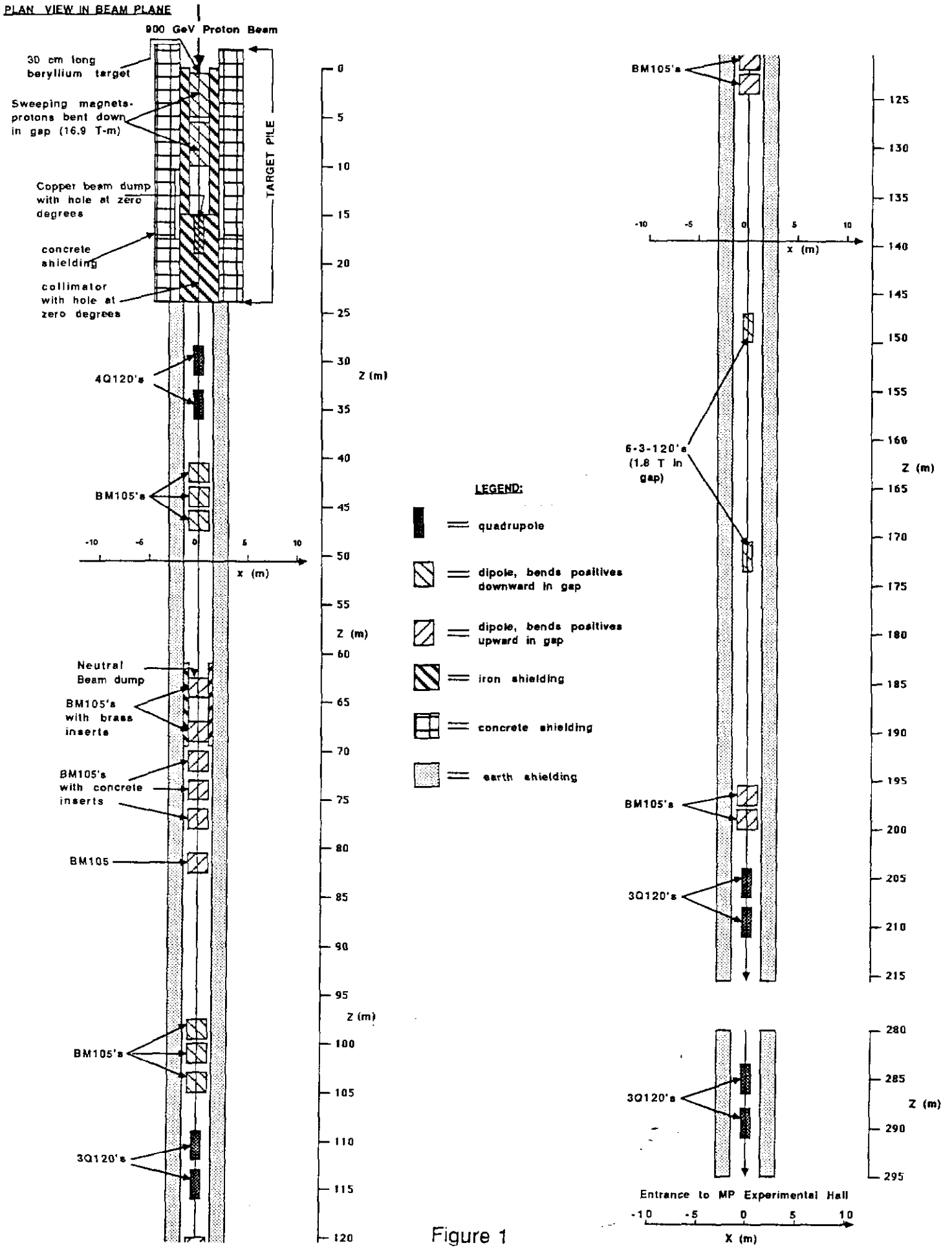
PLAN VIEW IN BEAM PLANE
900 GeV Proton Beam
30 cm long beryllium target
Sweeping magnets- protons bent down in gap (16.9 T-m)
Copper beam dump with hole at zero degrees
concrete shielding
collimator with hole at zero degrees
TARGET PILE
4Q120's
BM105's
Neutral Beam dump
BM105's with brass inserts
BM105's with concrete inserts
BM105
BM105's
3Q120's
x (m)
Z (m)
LEGEND:
quadrupole
dipole, bends positives downward in gap
dipole, bends positives upward in gap
iron shielding
concrete shielding
earth shielding
BM105's
6-3-120's (1.8 T in gap)
BM105's
3Q120's
3Q120's
Entrance to MP Experimental Hall
X (m)

Figure 1

CROSS SECTION AS MODELED AT Z = 8 METERS:

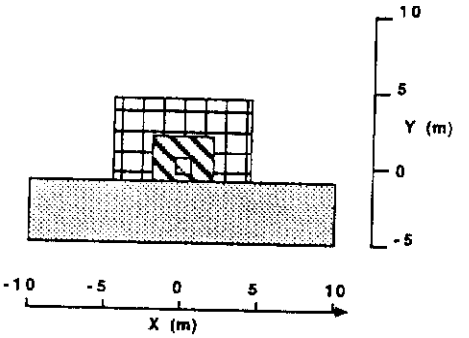

Definition of Quadrants

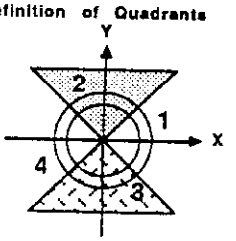

Figure 2

CROSS SECTION AT Z = 70 METERS:
(neutral beam dump)

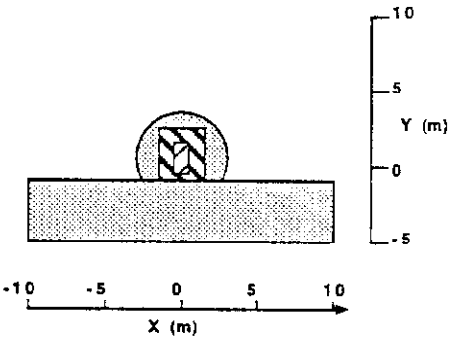

Definition of Quadrants:

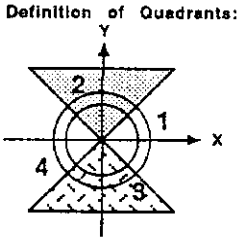

Figure 3

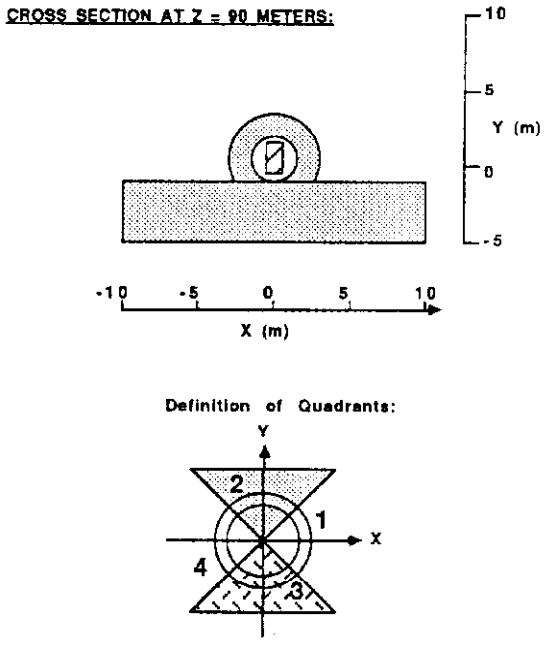

Figure 4

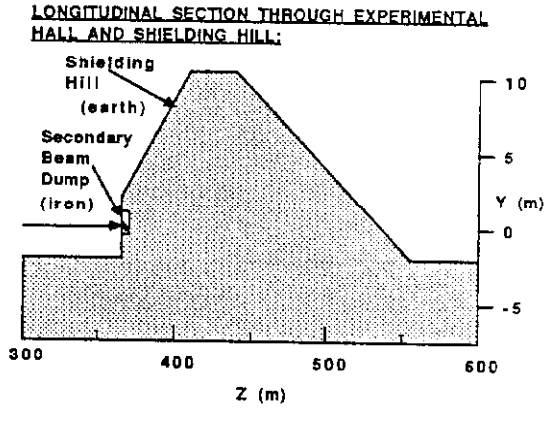

Figure 5

DETAIL OF SECONDARY BEAM DUMP:

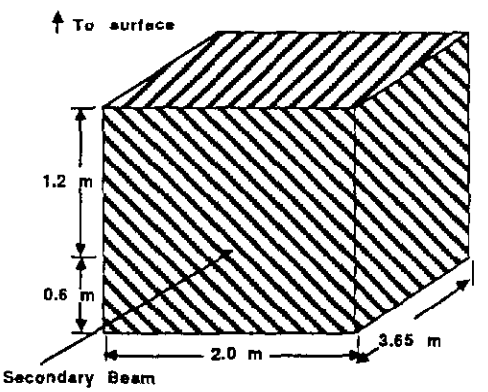

Figure 6

VIEW OF BM105 DIPOLE:

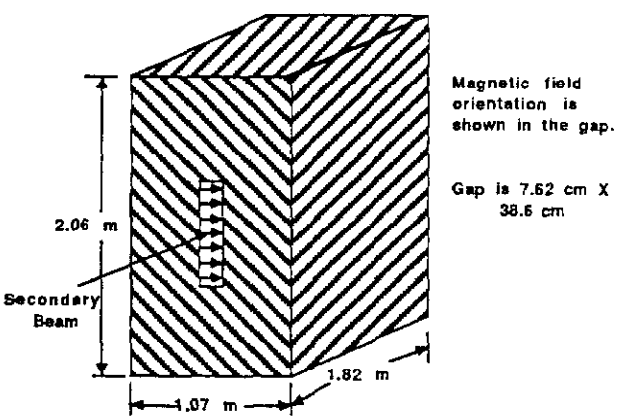

Figure 7

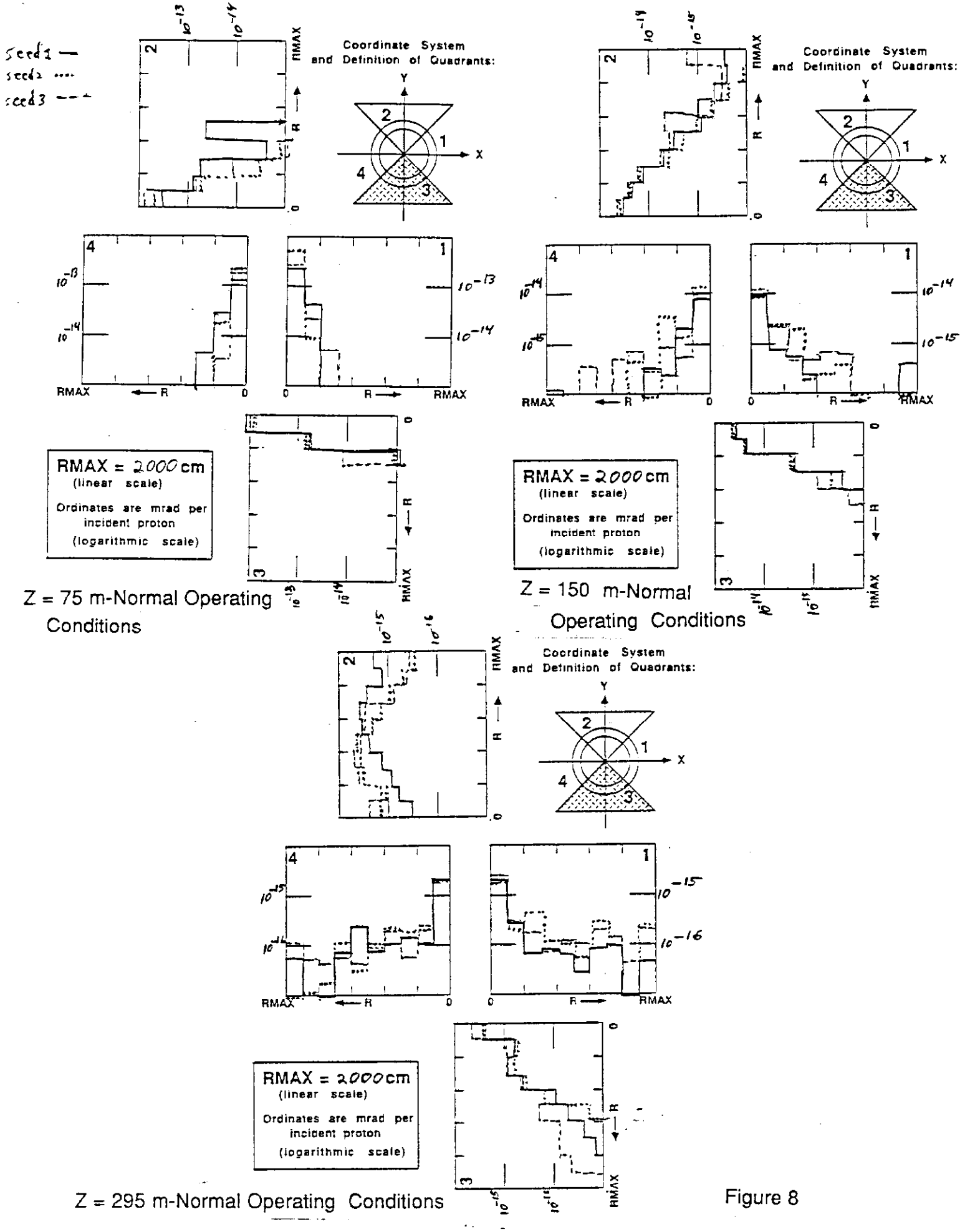
seed1
seed2
seed3
Coordinate System and Definition of Quadrants:
RMAX = 2000 cm
(linear scale)
Ordinates are mrad per incident proton
(logarithmic scale)
Z = 75 m-Normal Operating Conditions
Z = 150 m-Normal Operating Conditions
Z = 295 m-Normal Operating Conditions

Figure 8

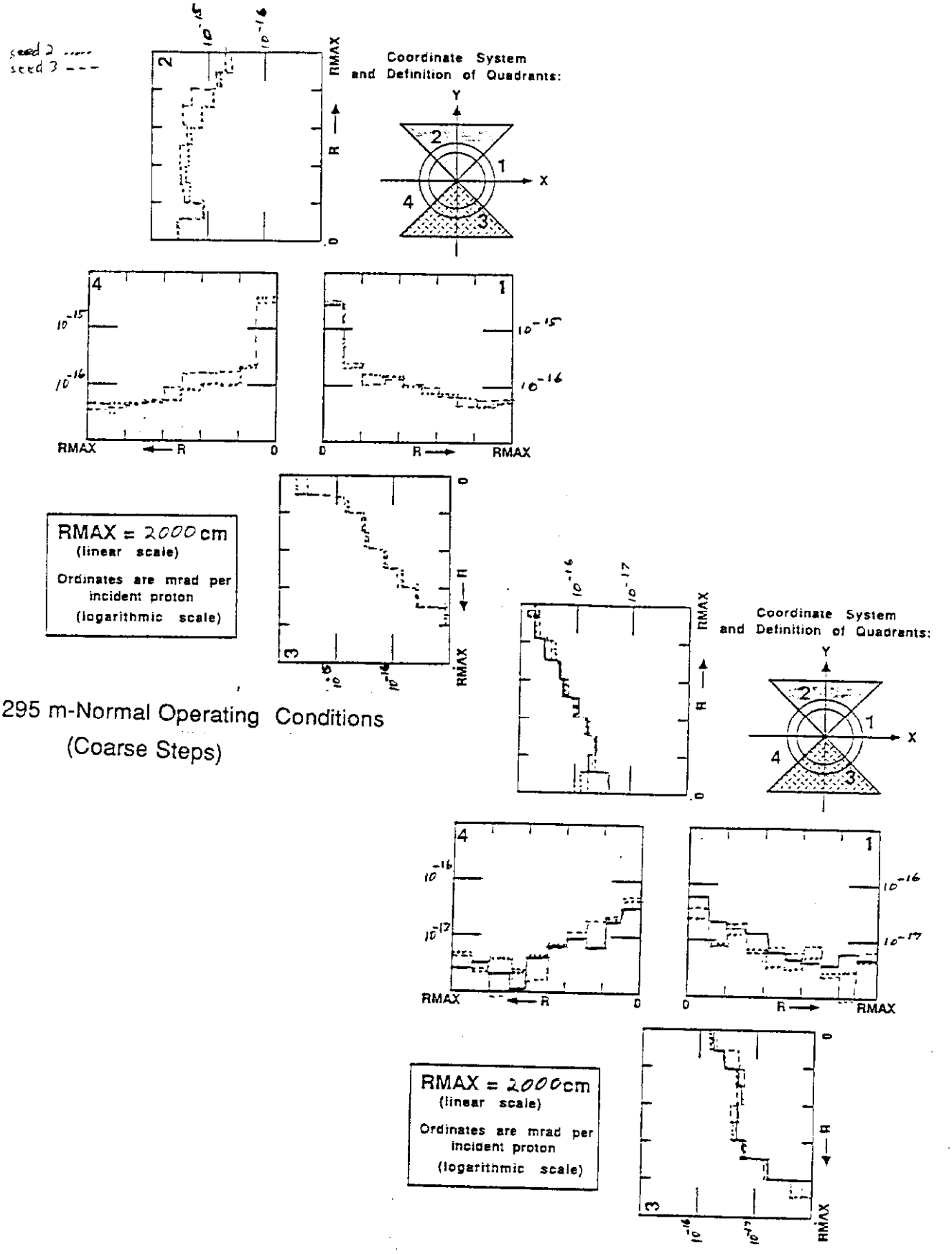
seed 2 ---
seed 3 - - -
Coordinate System and Definition of Quadrants:
RMAX
R
0
X
Y
RMAX = 2000 cm
(linear scale)
Ordinates are mrad per incident proton
(logarithmic scale)
Z = 295 m-Normal Operating Conditions
(Coarse Steps)
Coordinate System and Definition of Quadrants:
RMAX = 2000 cm
(linear scale)
Ordinates are mrad per incident proton
(logarithmic scale)
Z =590 m-Normal Operating Conditions (Coarse Steps)

Figure 9

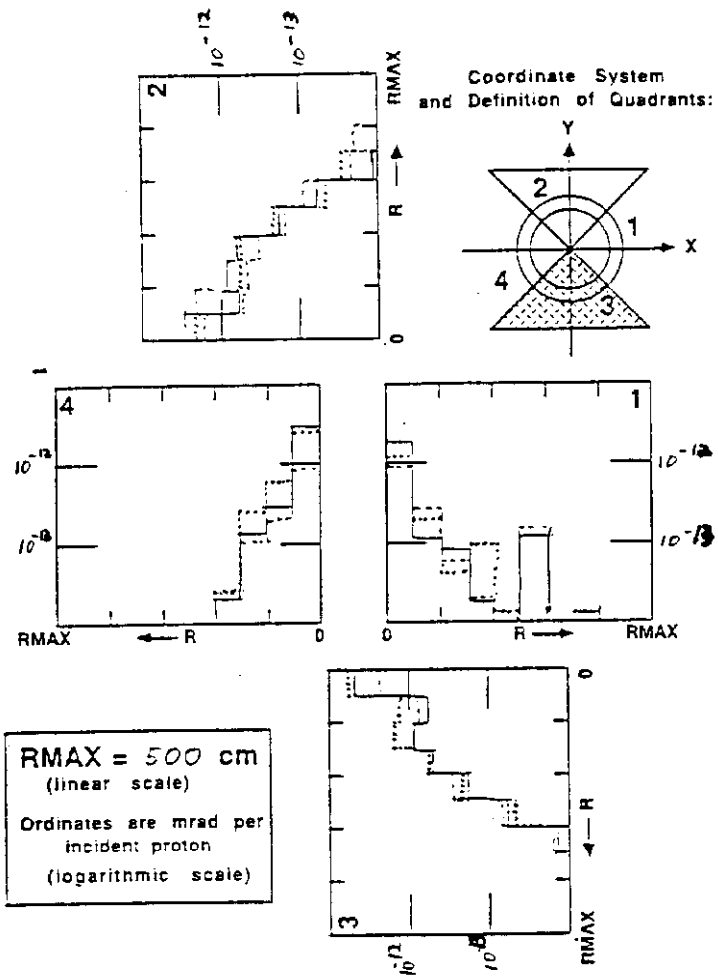

Z = 75 m-Normal Operating Conditions

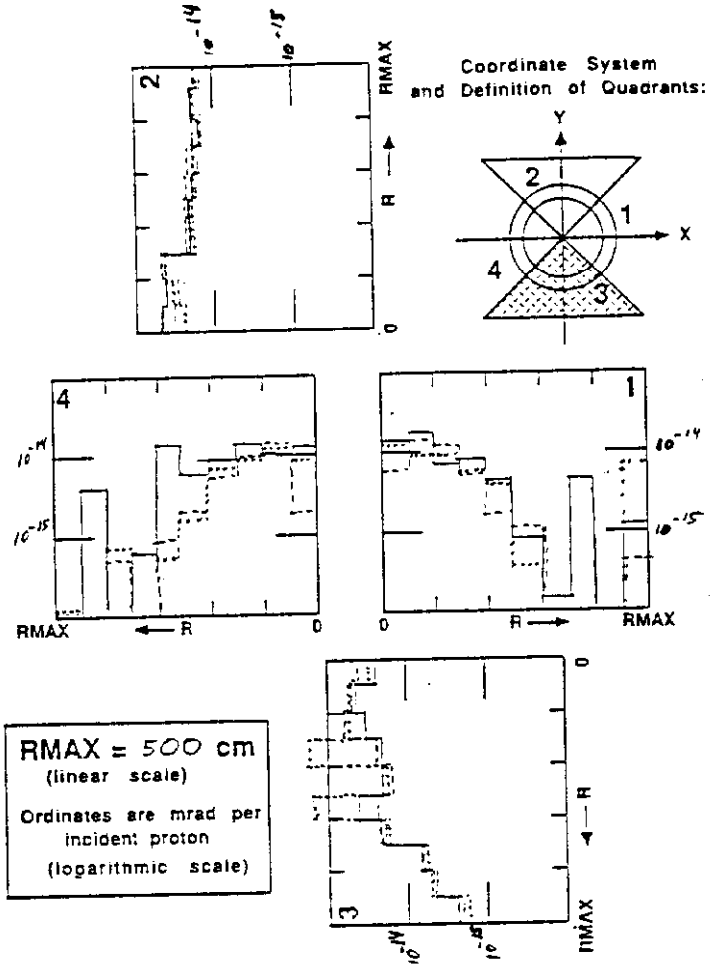

Z = 150 m-Normal Operating Conditions

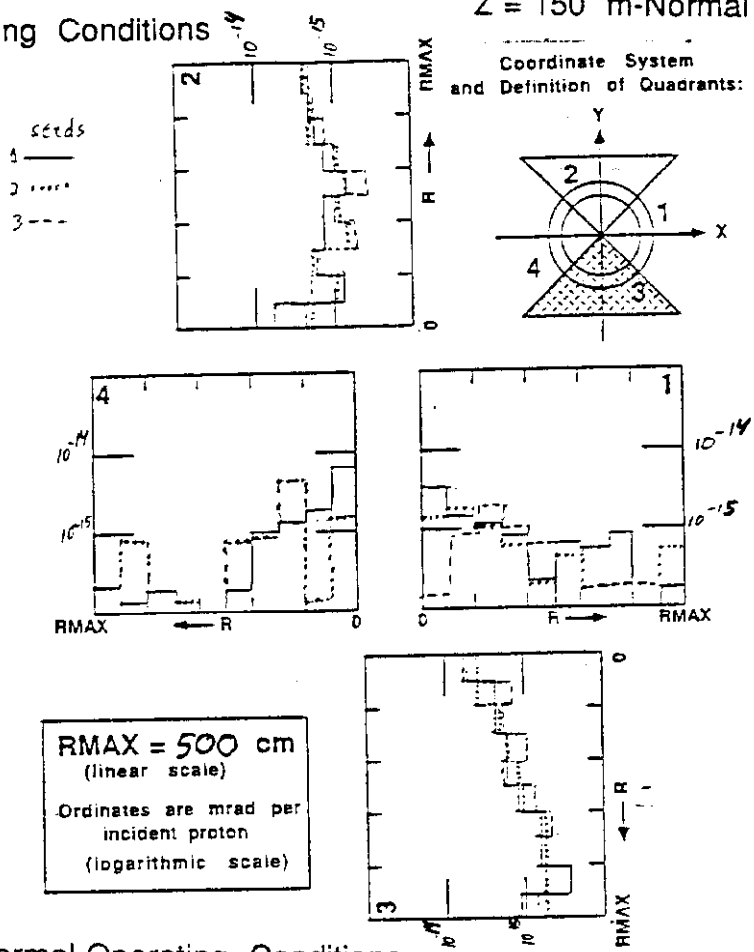

Z = 295 m-Normal Operating Conditions

Figure 10

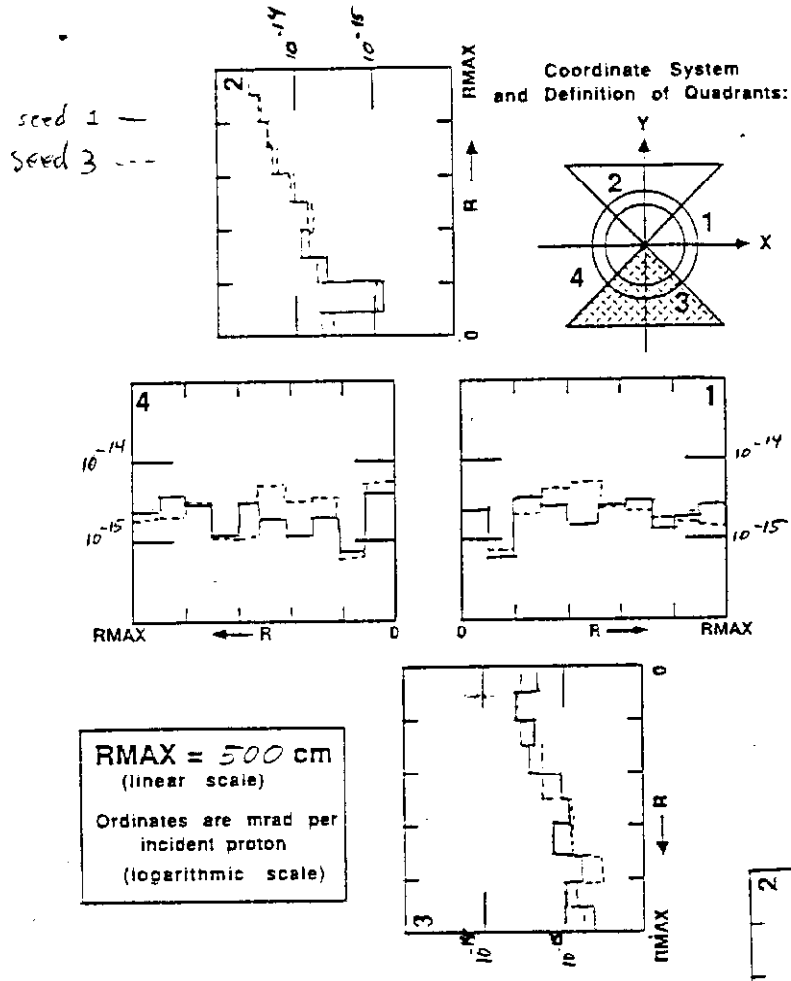

Z = 295 m-Normal Operating Conditions
Except With No Earth Berm

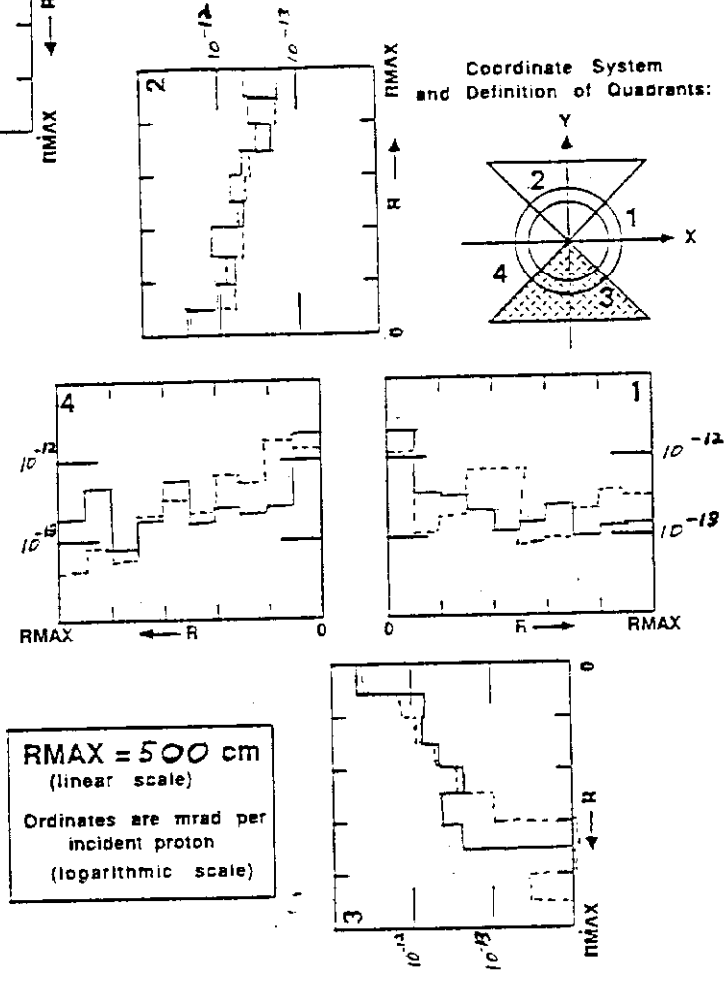

Z = 75 m-Normal Operating Conditions
Except With No Earth Berm

Figure 11

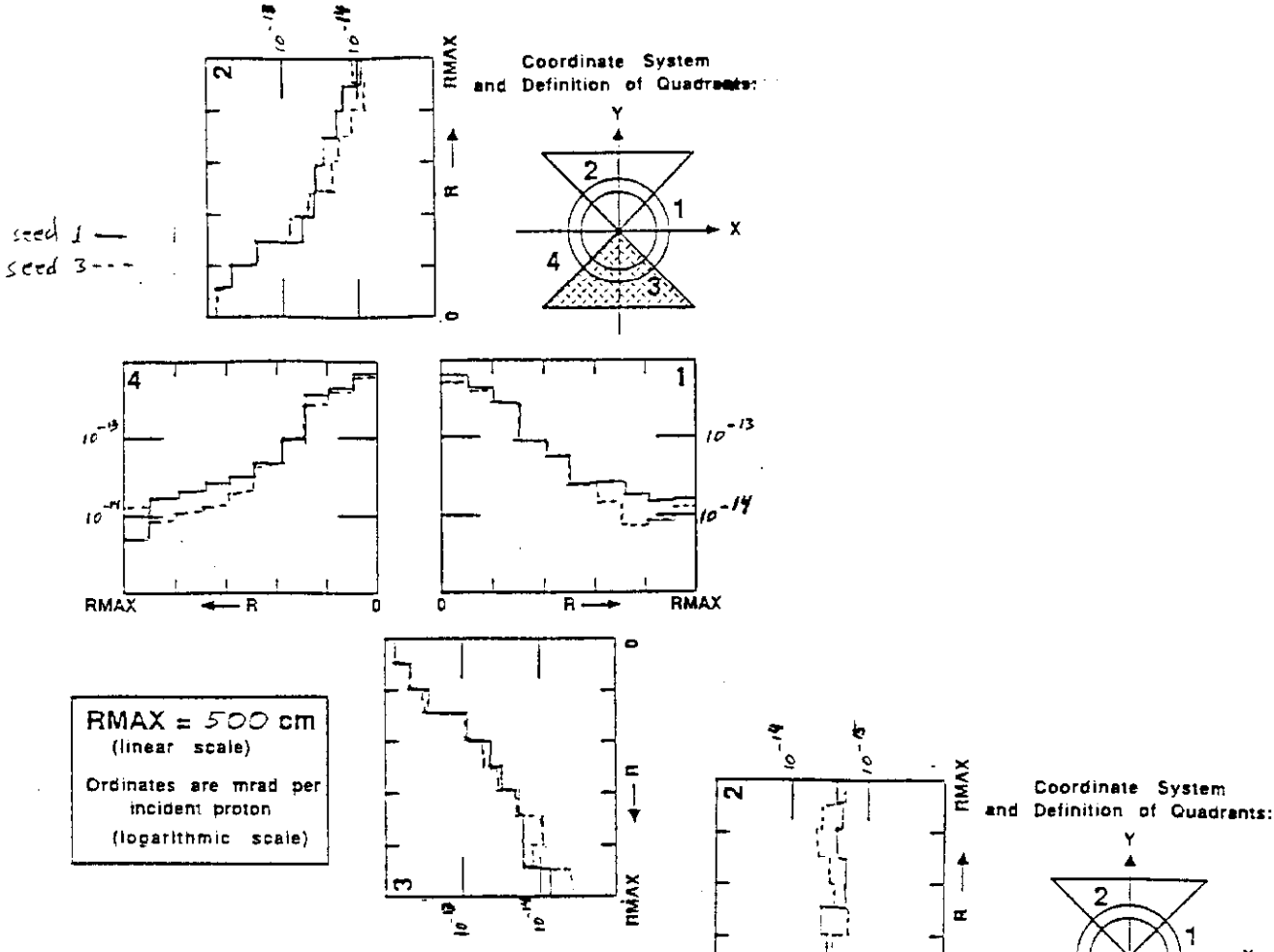

Figure 12 Z = 295 m-No Field in Dipoles

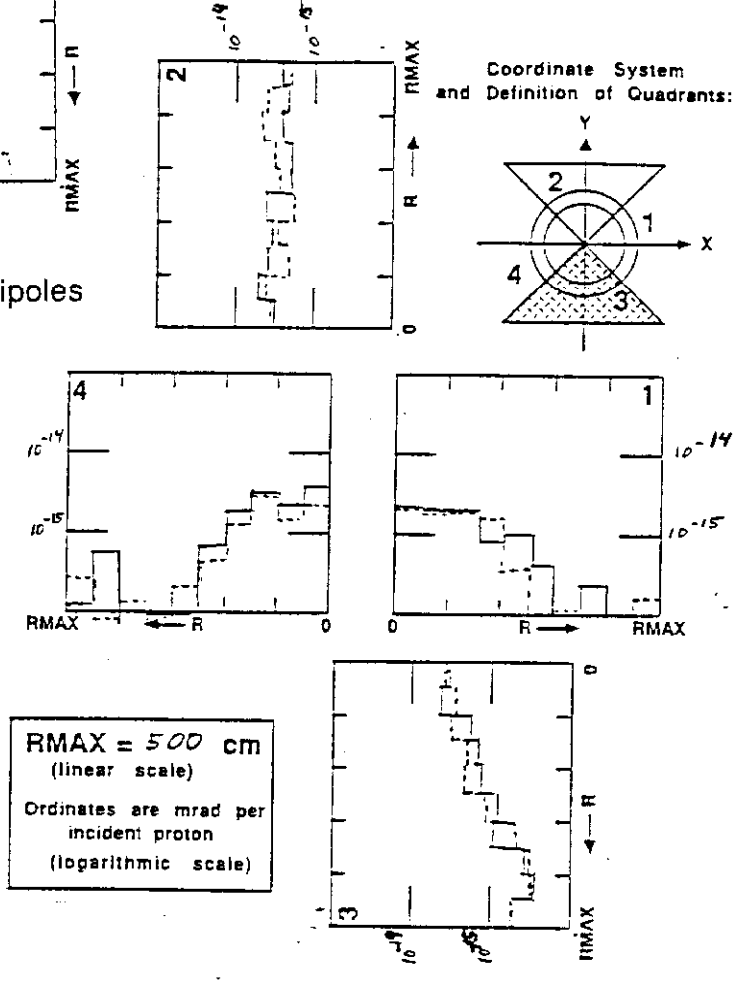

Figure 13 Z = 295 m-No Field in First Sweeping Magnet

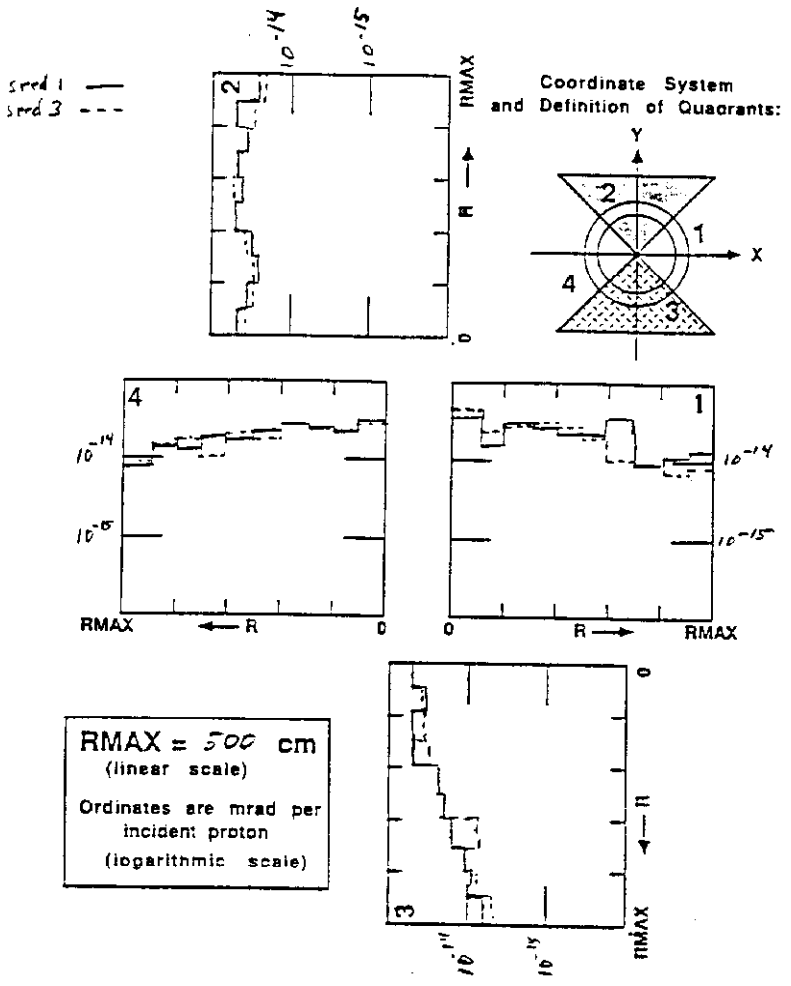

Figure 14 Z = 295 m-No Field in Either Target Pile Sweeper

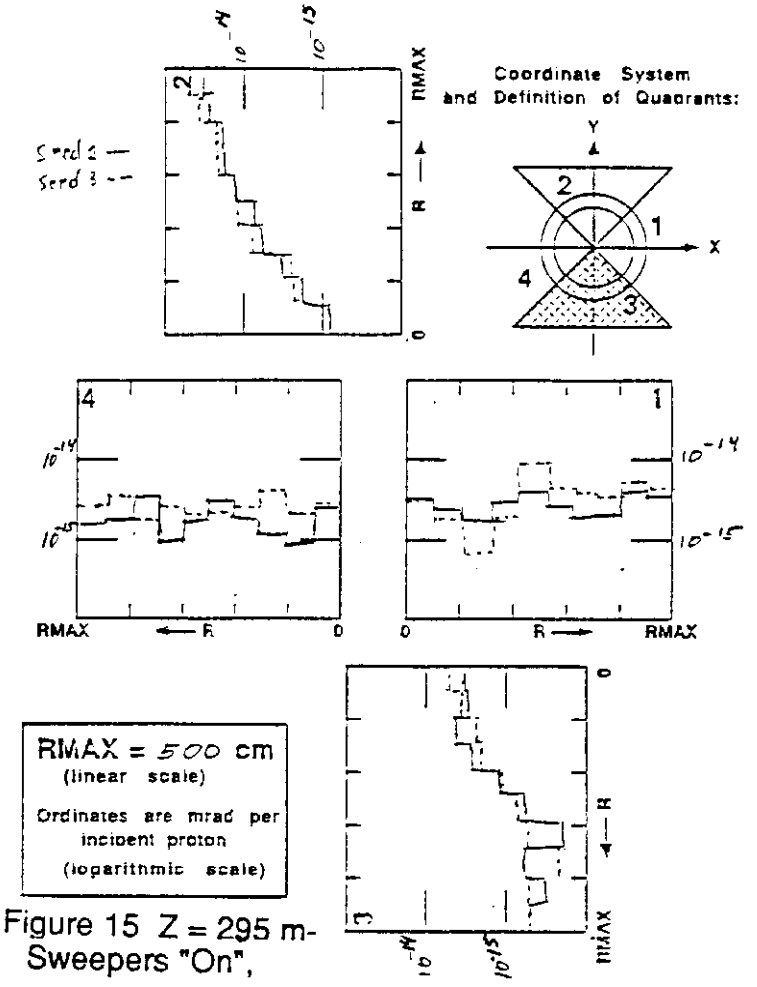

Figure 15 Z = 295 m-Sweepers "On", All Other Dipoles "Off"

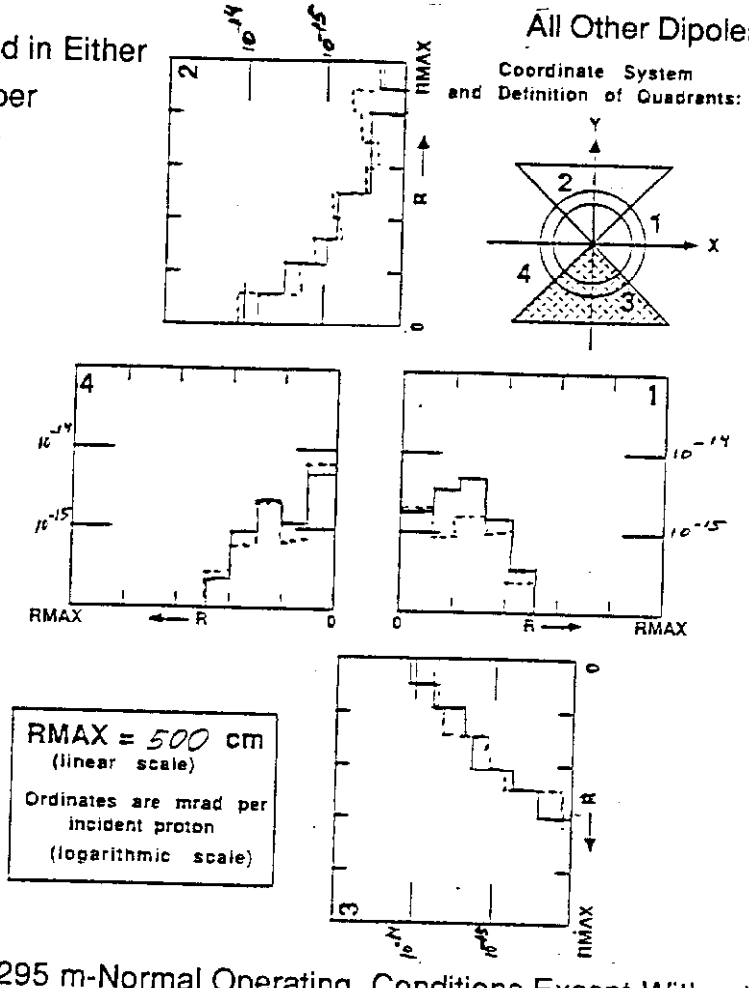

Figure 16 Z = 295 m-Normal Operating Conditions Except Without a Target